Electronic properties and hyperfine parameters of gold–3d-transition-metal impurity pairs in silicon

Lucy V. C. Assali and João F. Justo
Instituto de Física da Universidade de São Paulo, Caixa Postal 66318, 05315-970, São Paulo, SP, Brazil
(Received 29 January 1998)

We report theoretical investigations of the chemical trends in the electronic properties of transition-metal impurity pair complexes in a semiconductor. Self-consistent *spin-unrestricted* electronic state calculations, with a scalar relativistic scheme, in the framework of the multiple-scattering $X\alpha$ molecular cluster method, have been carried out for the substitutional gold-3d interstitial transition-metal pairs in silicon in C_{3v} symmetry. The role played by the 5d and 3d states of the transition metals in the formation of the impurity energy levels in the crystal band gap and resonances is established. The analysis of the one-electron energy spectra of the Au_sTi_i, Au_sV_i, Au_sCr_i, Au_sMn_i, Au_sFe_i, Au_sCo_i, and Au_sNi_i pair impurities leads to the conclusion that the electronic, magnetic, and optical properties of the series can be explained by a simple microscopic model. The calculations do not provide support for the ionic model, where these pairs are described as two point charges electrostatically bounded with a strong magnetic coupling between their spins. Instead, the results lead to a model in which the covalent effects are invoked to explain the chemical trends and the physical properties of the complexes. This model is substantiated by comparing the hyperfine parameters and transition energies with electron paramagnetic resonance and optical experimental data. [S0163-1829(98)08031-X]

I. INTRODUCTION

Complexes of point defects and/or impurities have been studied for many years using several experimental techniques. It has been found that complexes are formed by interacting impurities, inducing deep levels, resonances, and hyperdeep levels in the electronic structure of an otherwise perfect crystal. It has been well known for more than 30 years that the interstitial 3d transition metals are very mobile in silicon, even at room temperature, forming complex pairs with both shallow and deep impurities in silicon.[1]

Complexes involving gold and 3d transition metals in silicon have deserved particular attention. This is because gold, a deep impurity, is one of the most extensively investigated centers in silicon.[2–7] Electron paramagnetic resonance (EPR) experiments have attempted to establish a microscopic model for isolated gold in silicon. However, the experimental data pointed only to the existence of gold-related complexes.[1,8–14]

Recently, Zeeman studies of the donor and acceptor excitation spectra provided detailed information on the electronic structure of the neutral substitutional gold in silicon.[15,16] The center is paramagnetic ($S=1/2$) with $g_{\parallel}\approx 2.8$ and $g_{\perp}\approx 0$, and has a static $\langle 100\rangle$ tetragonal distortion (D_{2d}). This observation suggested that the $g_{\perp}\approx 0$ could be better explained by an increased spin-orbit interaction, as proposed to explain the missing EPR signal.[17] Moreover, the initial states in both the acceptor and donor excitation spectra were found to have the same structure.[15,16] This provides direct evidence that both spectra arise from the same defect since the optical energies match well the $E_c-0.55$ eV and $E_v+0.35$ eV levels attributed to the acceptor and donor levels, respectively, of the isolated gold center in silicon.[18–20]

In addition to the fascinating puzzle that isolated gold has provided during all these years, numerous experimental investigations provided a wealth of information on the nature of various centers related to gold in silicon, specifically the gold-transition metal pairs.[1,8–13] The charge states of the pairs have been controlled by the concentration of shallow acceptors or donors present in the sample. EPR technique was used to determine the effective spin and the structure of Au-TM complex defects.[1,8–11] Some complexes are associated with electrically active gap levels that have been characterized by diode capacitance measurements, including deep-level transient spectroscopy (DLTS).[12,13] EPR experiments showed that the pairs are aligned along the $\langle 111\rangle$ direction with a trigonal symmetry, indicating that they may consist of a substitutional gold with a TM impurity occupying a nearby interstitial site. Since the symmetry assigned to the pairs is trigonal, it seems that when the two species, the TM and Au impurities, are present in the sample, the isolated gold impurity moves from its distorted tetragonal configuration to a substitutional site to pair with the interstitial nearest-neighbor TM impurity.

An ionic model has been suggested to properly describe the EPR parameters of the positively ionized gold-manganese pair $(Au_s^- Mn_i^{2+})^+$ in Si.[1] This ionic model has been applied to describe some properties of gold-TM centers.[8–12] According to that description, the observed EPR signals come from a magnetic coupling between the angular momenta of the two isolated ions, one centered on the gold and the other on the TM impurity. Therefore, the notation $Au_s^- TM_i^+$ has been currently used to denote the pairs.

Previous calculations, using the multiple scattering method in the *spin-restricted* treatment, and without scalar relativistic inclusion, for Au_sFe_i and Au_sMn_i pairs, provided no support for the ionic model, showing that the pair impurity levels arise from an interaction between the molecular orbitals of the isolated impurities and the Si host atoms.[21,22]

In this investigation we address the problem of modeling

0163-1829/98/58(7)/3870(9)/$15.00 PRB 58

the microscopic structure of Si:Au$_s$$TM_i$ trigonal centers, with TM=Ti, V, Cr, Mn, Fe, Co, and Ni to study the chemical trends in the electronic properties along the 3*d* series. Moreover, we move a step forward by carrying out the self-consistent simulations to the *spin-unrestricted* limit, using scalar relativistic theory. This formalism is essential for a proper comparison with experimental properties, such as the total spin and the position of energy levels in the gap. The Fermi hyperfine contact fields at the Au$_s$, TM_i, and Si nuclei are evaluated and compared to available EPR results. Besides, the Mott-Hubbard energies are compared to experimental donor and acceptor transitions measurements obtained by DLTS. The paper is organized as follows: in Sec. II we present the theoretical model, and in Sec. III we present the electronic structure for the Au$_s$$TM_i$ trigonal complexes in Si, including the Fermi contact fields and the Mott-Hubbard potentials for the centers. Finally, in Sec. IV we present final remarks.

II. THEORETICAL MODEL

The calculations were carried out within the framework of the molecular cluster model. Initially, a 26 Si-atom cluster, centered at the tetrahedral interstitial site, was adopted in order to define the band edges of the perfect silicon cluster that simulates the crystal. The values of 1.4 eV and 10.2 eV were obtained for the material energy band gap and valence-band width, respectively. The symmetries of the energy levels in the self-consistent-field (SCF) electronic structure of the perfect cluster are in agreement with those expected by group theory. The cluster energy-band-gap (valence-band-width) value certainly decreases (increases) when larger size clusters are considered, as has been discussed previously.[23] However, the study of the chemical and physical properties of impurities using the cluster model is not expected to change if cluster size changes. Therefore, this perfect cluster provides a good reference system to simulate the electronic properties of deep defects and/or impurities.

All complexes analyzed were considered in a configuration where one impurity replaces a silicon host atom (Au$_s$) and the other sits in a nearest-neighbor interstitial tetrahedral site (TM_i). The defect pairs are surrounded by 25 Si atoms such that the clusters have a $\langle 111 \rangle$ trigonal C_{3v} symmetry.

The one-electron Schrödinger equations were solved for the molecular cluster by using the *ab initio spin-unrestricted* multiple-scattering theory developed by Johnson and Slater[24,25] with $X\alpha$ statistical exchange potential.[25]

The muffin-tin atomic spheres were chosen such that they touch each other and have the same radii, consistent with the Si interatomic distance (2.352 Å).[26] In the atomic region the Schwarz exchange parameters (α) were used.[27] Simulations using either the Hedin-Lundqvist[28] or Ceperly-Alder[29] approximations, to the exchange potential, showed that the results are qualitatively independent of the exchange potential used, even in the *spin-unrestricted* case. The sphere that surrounds the whole cluster touches its surface atomic regions and is made to coincide with a Watson sphere, which is used to neutralize the effects of the dangling-bond surface states, as proposed by Fazzio *et al.*[30] This method has been used successfully to describe the electronic structure of complexes in semiconductors.[21,22,31,32]

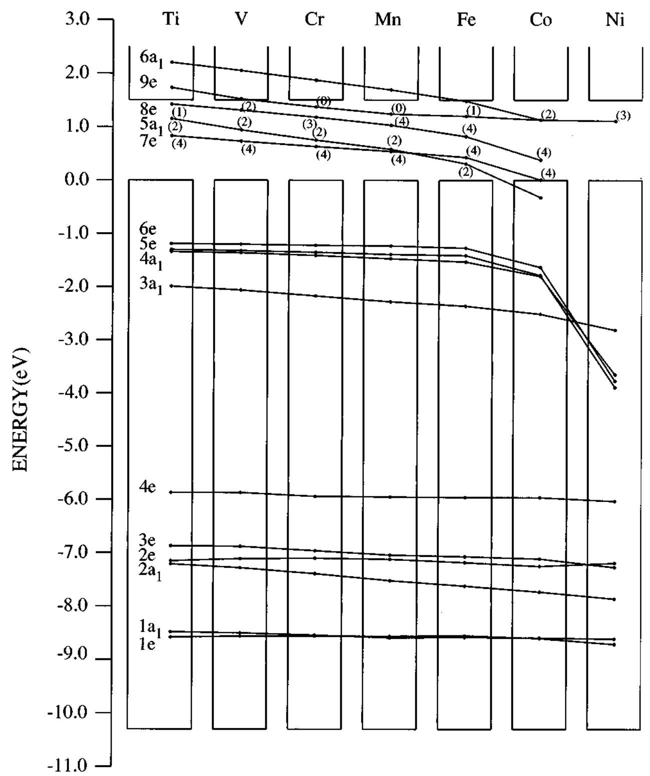

FIG. 1. Self-consistent one-electron spectra for 25Si+Au$_s$$TM_i$ (TM=Ti, V, Cr, Mn, Fe, Co, and Ni) clusters simulating the electronic structure of neutral Au$_s$$TM_i$ trigonal complexes in crystalline Si. The figure only displays the gap levels, the gold-5d, and TM-3d-related energy levels. The occupancy of the gap levels is indicated by numbers in parentheses, and resonances inside the valence and conduction bands are assumed to be completely filled or empty, respectively.

All electrons were considered in the simulations, meaning that there are no frozen cores. The basis set for the expansion of the wave functions included values up to $l=2$ for the outer region, TM, and Au atoms, and up to $l=1$ for the silicon atoms. It is worth mentioning that lattice relaxations and distortions were not taken into account. On the other hand, scalar relativistic theory was used since it is important in describing core orbitals. In this approach, the radial functions inside each atomic sphere satisfy an average Dirac equation that includes the Darwin and mass-velocity corrections.[33,34] Such corrections affect all of the energy levels since the calculations are self-consistent, including important direct and indirect level shifts.

III. RESULTS AND DISCUSSIONS

A. Spin-restricted electronic structure of the neutral Si:Au$_s$$TM_i$ systems, with TM=Ti, V, Cr, Mn, Fe, Co, and Ni

To understand the chemical trends in the electronic properties displayed by the systems, it is useful to first analyze the results obtained for the *spin-restricted* electronic structure of the Au$_s$$TM_i$ pairs in silicon.

Figure 1 shows the self-consistent one-electron results for the 25Si+Au$_s$$TM_i$ cluster simulating the electronic structure of Au$_s$Ti$_i$, Au$_s$V$_i$, Au$_s$Cr$_i$, Au$_s$Mn$_i$, Au$_s$Fe$_i$, Au$_s$Co$_i$, and Au$_s$Ni$_i$ trigonal complexes in silicon. The figure only displays energy levels that play a fundamental role in determining the physical properties of the complexes and are important to understand the chemical trends along the series. The band edges were defined according to the energy spectrum of the 26 Si-atom cluster, which simulates the crystal, and the energy zero is set at the valence-band maximum. The calculations were carried out with all the levels filled according to the ordering of increasing energy. The occupancy of the gap levels is indicated by numbers in parentheses and resonances inside the valence and conduction bands are assumed to be completely filled or empty, respectively. Calculations for the Au_sCu_i complex were also performed. The electronic structure spectrum shows a peculiar behavior related to the $3d$-$5d$ molecular orbitals interaction as resonant energy levels in the silicon valence band, differently from the pairs analyzed here. Therefore, we present the results related to complexes involving Cu in a forthcoming publication.

The analysis of the results depicted in Fig. 1 leads to the conclusion that the electronic properties of the pairs can be described by bearing in mind that the complex impurity levels come from a covalent interaction between the molecular orbitals of the isolated impurities, split by a trigonal crystal field, for all $3d$ series, consistent with previous calculations for the Au_sFe_i and Au_sMn_i impurities in trigonal symmetry.[21,22]

Neutral Au_s in Si gives rise to a threefold degenerated t_2 level in the band gap, occupied by three electrons and $5d$-derived resonances fully occupied.[35,36] According to Alves *et al.*,[35] using the multiple-scattering method, the Au_s $5d$ states give rise to $e(d)$ and $t_2(d)$ hyperdeep energy levels induced close to the bottom of the valence band, while according to quasiband crystal field (QBCF) calculations[36] the $5d$ states are located in the lower part of the valence band and the $t_2(d)$ level (labeled as t_2^{CFR}) displays a width of about 1.0 eV. The t_2 gap level is called a *dangling-bond-like* state in the case of cluster computational simulations and *dangling-bond hybrid* in the QBCF results.

In order to explain the electronic properties of the stabilized pairs, we propose a model as derived from interactions between the molecular orbitals of the isolated impurities. Therefore, we simulate the electronic structure of the isolated substitutional gold impurity in silicon using scalar relativistic theory to provide a better basis to analyze the results of the complexes exposed here.

The results of the calculations, using the same cluster described in Ref. 35, show a t_2 dangling-bond-like energy level in the gap, occupied by three electrons, as before, with a p-d hybrid character (5% of the charge in the Au sphere), but differently, the $5d$-derived orbitals give rise to a very compact $e(d)$ level ($E_v-6.15$ eV; electronic configuration $5d^{3.7}$) and two t_2 energy levels ($E_v-8.80$ eV and $E_v-6.15$ eV; electronic configuration $5d^{5.4}$). Besides, there is an a_1 resonant level ($E_v-1.53$ eV; electronic configuration $6s^{0.5}$), which could be compared to the a_1^R level found in the electronic structure of substitutional gold by Fazzio *et al.*[36] Therefore, it seems that the differences between the calculations mentioned above are due to the lack of relativistic theory approach and not due to cluster boundary conditions.[36]

The first interesting chemical trend in the electronic structure of the pairs is the localization of the gold $5d$-derived resonances observed along the series. These fully occupied levels come from the splitting by the C_{3v} crystal field of the $e(d)$ and t_2 resonant levels induced in the silicon valence band by the substitutional gold impurity, as discussed before, and are labeled as $1e$, $1a_1$, $2a_1$, $2e$, $3e$, and $4e$ in Fig. 1. The perturbation caused by the TM impurity in the gold t_2 and $e(d)$ resonant levels is small, so that the $5d$-derived levels remain regularly as resonances in the valence band along the series. The interaction between these states and the silicon host states gives rise to another resonance of e symmetry. The a_1 resonant gold energy level appears in the complexes and is labeled as $3a_1$ in Fig. 1. It has a silicon valence-band-state character, showing a weak interaction between $Au-6s$ and TM atomic orbitals.

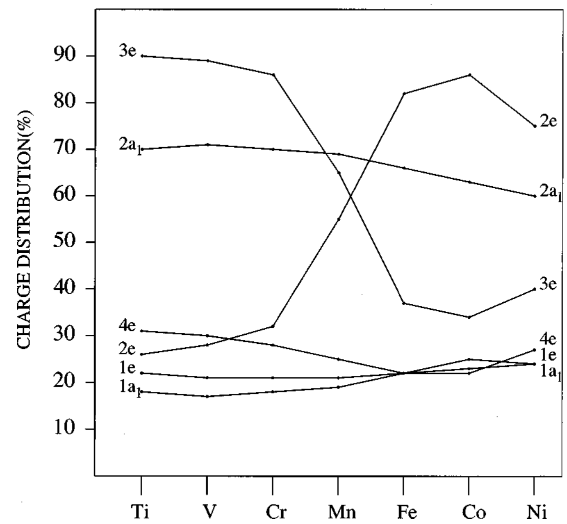

FIG. 2. Percentage of charge (normalized to one electron) inside the Au_s sphere for the $5d$-related levels in the neutral Au_sTM_i trigonal complexes in Si. These levels are labeled according to Fig. 1.

The electronic charge in the Au_s sphere for the $5d$-related levels is shown in Fig. 2. For all complexes the electronic configuration of these orbitals is about $5d^{9.1}4s^{0.4}$. We conclude that the gold $5d$- and $4s$-derived states play a minor rule in determining the pair complexes' electronic properties.

The $9e$ and $6a_1$ energy levels, shown in Fig. 1, have a charge distribution that is mostly localized in the gold first- and second-neighbor silicon atoms and result from the crystal-field splitting of the substitutional gold t_2 dangling-bond-like gap level when the symmetry is lowered from Td for the Au_s to C_{3v} for the Au_sTM_i complexes. We will discuss them later.

We now analyze the trends displayed by the TM impurity-induced levels that originate from the $3d$ atomic states, appearing as resonances within the valence band and as impurity levels in the gap.

An isolated tetrahedral interstitial $3d^n4s^2$ TM_i impurity gives rise to $3d$-derived states within the valence band and as impurity levels in the gap, with t_2 and e symmetries.[37–39] In the C_{3v} crystal field of the pairs, the $3d$-derived states lead to a nondegenerate a_1 level and a pair of twofold degenerate e levels. The $3d$-derived resonances in the valence band are described by the electronic configurations $6e$, $5e$, and $4a_1$. The TM_i $3d$-derived gap states are labeled as $7e$, $8e$, and

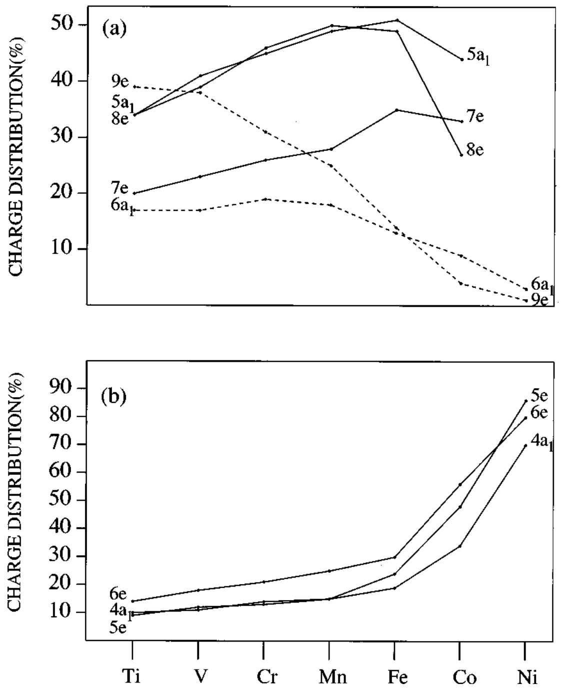

FIG. 3. Percentage of charge (normalized to one electron) inside the TM_i spheres in the neutral Au_sTM_i trigonal complexes in Si: (a) $3d$-derived gap levels (full lines) and Au_s t_2-derived dangling-bond-like levels (dashed lines); (b) $3d$-derived valence resonance levels. All the levels are labeled according to Fig. 1.

$5a_1$ in Fig. 1 and are complemented by the results displayed in Figs. 3(a) and 3(b), which show the probability of finding an electron in the TM_i spheres for each of these states.

As in the case of the isolated tetrahedral interstitial Ni impurity,[37] for the Au_sNi_i pair there are no gap levels with $3d$ character. The electrons in $7e$, $8e$, and $5a_1$ states for the Au_sNi_i complex have a valence-band-state character and are not shown in Fig. 1, while those occupying the $6e$, $5e$, and $4a_1$ states are highly localized in the Ni atom and are resonant energy levels in the valence band. The $9e$ and $6a_1$ gap levels are degenerated and are typical dangling-bond-like states. As one proceeds to lighter impurities, the $3d$ orbitals of the TM_i atom interact with the host states and push the a_1 and e levels towards the band gap. When Ni is replaced by Co, the electrons in the resonance states begin to delocalize while the $7e$, $8e$, and $5a_1$ orbitals show a $3d$ character. When Co is replaced by Fe, the interaction between the impurities increases, the crystal field splits the energy level derived from the substitutional gold t_2 dangling-bond-like orbitals into $9e$ and $6a_1$ energy levels, and the charge distribution of these levels begins to display a $3d$ character while the resonant levels begin to delocalize, as can be seen in Fig. 3. This trend continues through the TM_i series, so that going from Ni to Ti, the resonance states delocalize onto the neighboring silicon atoms.

As one proceeds from heavier to lighter impurities, the $3d$ states interact with the host states and move up into the valence band. Due to hybridization with valence states, the $3d$-derived resonances become progressively more delocalized. We observe the striking similarity between the chemical trends of the $3d$-derived impurity levels for the pairs and for the TM_i impurities themselves.[37–39]

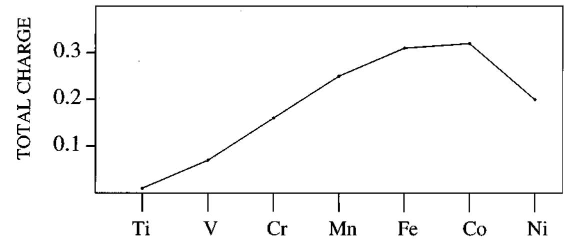

FIG. 4. Net electronic charge inside the TM_i spheres for the neutral Au_sTM_i trigonal complexes in Si.

The feature that emerges from the calculations is that the results do not provide support for the ionic model. This conclusion, already reached for the Au_sFe_i and Au_sMn_i pairs,[21,22] is here extended to all components in the series. The values of the net electronic charge inside the TM_i spheres, displayed in Fig. 4, show clearly that there is no charge transfer from the TM_i atoms to the Au_s impurity. The values are systematically larger than the corresponding atomic numbers of the TM impurities. Such charge excess could be attributed in part to the small size of the impurity atoms and the large muffin-tin sphere they occupy. This is not the case here since the muffin-tin-spheres radii are equal to 1.18 Å, much smaller than the atomic radii of the TM atoms and of the same order of the covalent radii of these impurities. Here the Haldane and Anderson mechanism,[40] which is inherent in our covalent model of the complexes, keeps the net charge inside the TM_i sphere approximately neutral. Therefore, the differences between electronegativity of the elements in the pair are not a reliable criterion to analyze charge-transfer effects for impurities in semiconductors.[8]

The ionic model is based on the idea that the TM_i atoms, acting as donor impurities, are charged positively in compensated samples and a related number of acceptor impurities are charged negatively. The pairing occurs due to the interaction between the two ions. This hypothesis could be valid for the tetrahedral interstitial Ti, V, Cr, and Mn impurities, which are associated to donor transition levels[41] placed above the Au_s acceptor level at $E_c - 0.55$ eV.[18–20] It could also be a reasonable hypothesis to explain the pairing between the TM_i impurities and the typical isolated shallow acceptor centers. However, this model would not explain the existence of the stable Au_sFe_i pair. Interstitial isolated iron has only one well established donor level at $E_v + 0.385$ eV,[41] therefore it is below the acceptor level of gold, avoiding the possibility of a configuration such as $Au_s^- Fe_i^+$ for the pair.

The overall analysis of the charge distribution in Figs. 2 and 3, associated to the one-electron spectra shown in Fig. 1 and complemented by Fig. 4, that shows the total charge inside TM_i spheres, allows us to conclude that the pairs are formed by a covalent mechanism that includes, besides Au_s and the TM_i impurities, also the silicon neighbors. Therefore, the EPR parameters of the pairs should be related to molecular orbitals spread out over the cluster rather than being derived from the interactions between two localized magnetic centers, as has been assumed.[8–12] We also point out that the ionic notation $Au_s^- TM_i^+$ for all of the complexes is misleading.

From Fig. 1 it can be verified that the $9e$ and $6a_1$ are the only levels in the gap for the Au_sNi_i complex. As one proceeds to lighter TM impurities, two effects occur simultaneously. The $8e$ level moves up, becoming closer to the $9e$ level and the $3d$ composition of the $9e$ level increases. From Fig. 3(a) it can be verified that the gap levels behave as typical dangling-bond-like states for the Au_sNi_i and Au_sCo_i pairs and as typical TM_i $3d$ states for Au_sMn_i, Au_sCr_i, Au_sV_i, and Au_sTi_i complexes. Therefore, it is expected that the former systems would behave as an isolated Au_s impurity and the latter as an isolated interstitial $TM-3d$ impurity, both in a trigonal crystal field. Although there is a non-negligible $3d$ contribution for the $9e$ state of the Au_sFe_i pair, the energy difference between the $9e$ (almost) dangling-bond-like level and the $8e$ $3d$-derived level is the most important quantity to evaluate whether the exchange splitting between states of opposite spin is larger than the crystal-field splitting (high spin configuration) or lower than the crystal-field splitting (low spin configuration), as has been suggested.[21]

Comparing the results presented in Fig. 1 for the electronic structure of the Au_sFe_i and Au_sMn_i complexes with those obtained previously,[21,22] two major differences are observed. First, the energy levels related to Au_s $5d$ orbitals are shallower in the valence band. Second, the trigonal crystal-field splitting in the Au_s t_2-dangling-bond-like gap level, resulting in the $9e$ and $6a_1$ energy levels, is smaller here than in those previous calculations. The differences are due to the use of scalar relativistic theory and the nonexistence of frozen core electrons in the present calculations.

Before exposing the *spin-unrestricted* electronic structure of Si:Au_sTM_i centers, with $TM=$Ti, V, Cr, Mn, and Fe, let us first discuss the *spin-restricted* electronic structures of the Au_sCo_i and Au_sNi_i pairs in silicon. Figure 1 shows that their properties are defined by the $9e$ and $6a_1$ gap states, the highest occupied energy levels in the spectra. We interpreted these results as the pairs having properties quite similar to those displayed by the isolated substitutional Au center. This is supported by the results displayed in Fig. 3(a), which show that these two levels and the t_2 gap state, in the isolated Au_s impurity, have analogous dangling-bond-like nature. Based on this, we could say that the main role played by the nearest-neighbor Ni_i impurity in the complex is to lower the crystal field ''*felt*'' by Au_s. In the case of the Au_sCo_i pair, the Co_i impurity also decreases by one electron the occupation of those levels coming from the Au_s gap level. However, this decrease does not necessarily imply in an ionic interaction between Au_s and Co_i, since the rearrangement of charge prevents charge transfer. As can be seen in Fig. 4, the total SCF charge inside the TM_i sphere does not increase by one electron as a result of the interaction.

It is worth mentioning that during the simulations, in which two or three electrons were accommodated in the $9e$ energy levels, for Au_sCo_i and Au_sNi_i, respectively, it turned out that their energies moved up higher than the $6a_1$ levels, during self-consistent cycles. On the other hand, if two electrons were accommodated in $6a_1$ levels, and zero (or one) in the $9e$ energy levels, the former moved up higher in energy than the $9e$ states, preventing convergence in the self-consistent cycles. Thus, the usual procedure of occupying the energy levels by integer numbers, according to the ordering of increasing energy, leaving all lower levels occupied and all higher levels empty, is not possible in these cases. Therefore, we have assigned fractional number of electrons to each of the two states, choosing the occupancy in order to make the two energy eigenvalues degenerated, as shown in Fig. 1. The degenerated nature of the $9e$ and $6a_1$ energy levels stems from a very small interaction between the impurity molecular orbitals, which is not strong enough to lower the degeneracy of the Au_s-t_2 dangling-bond-like gap level. This degeneracy remained even when simulating longer or shorter distances (in the $\langle 111 \rangle$ direction) between the TM_i and Au_s impurities.

Since the electrons filling these two degenerated energy levels are occupying delocalized states, the angular momentum is expected to be quenched and an effective low spin configuration can be ascribed to the ground state of the complexes, so that Au_sCo_i and Au_sNi_i pairs in Si have $S=0$ and $S=1/2$ values for the total spin, respectively, making *spin-polarized* simulations useless. Moreover, they are not likely active Jahn-Teller (JT) centers due to the delocalized character of the $9e$ and $6a_1$ states. Therefore, distortions are expected to be small and the Haldane and Anderson[40] mechanism is not operative.

By using the Slater procedure,[25] we evaluated the total energy differences between the *spin-restricted* and unrelaxed electronic configurations in order to obtain the donor $(0/+)$ and acceptor $(-/0)$ transition energies related to the pairs. The difference between donor and acceptor energies is defined as the Mott-Hubbard potential (U). The one-electron final states of the donor $(+/0)$ and acceptor $(-/0)$ transitions, as for the isolated gold center, are related to quite delocalized impurity states. For both centers the Mott-Hubbard energies are of the order of 0.4 eV, higher than the value of that assigned to isolated substitutional Au in silicon (0.22 eV).

The Au_sCo_i pair in silicon has not been experimentally identified yet. However, there are indications that Co, being a fast diffuser in silicon, may be involved in the formation of complexes.[41] Using DLTS measurements, Czaputa[13] observed two peaks correlated to Au-Ni complex in silicon, both of them with a donor character, corresponding to charge transition energies of $E_v+0.35$ eV and $E_v+0.48$ eV, exhibiting a bistable behavior. It was suggested that the complexes may consist of Au_s and Ni_i in two different positions, possibly nearest neighbor and next-nearest neighbor, representing the two bistable configurations. However, the stabilization of the pair could not be explained by an ionic interaction, since this model leads to contradictory conclusions when the Fermi level, in p-type Si, is considered.[13] Our results provide an explanation for why the Au-Ni complex can exist. An ionic interaction between the impurities is not required to keep the pair stable, even though the driving force to form the pair cannot be obtained by our static model. Therefore, it is possible that the pairing between a TM atom and an isolated impurity does not necessarily require the latter to be an acceptor center.

The pairs formed by the other atoms in the series (Ti, V, Cr, Mn, and Fe) have $3d$-derived energy gap levels, such that the *spin-unrestricted* simulations are important to better characterize their electronic structure. The results are present in the following sections.

TABLE I. Ground-state electronic properties of neutral, positive, and negative $\mathrm{Au}_s TM_i$ trigonal complexes in Si using the *spin-unrestricted* model. N is the total number of electrons filling the five highest energy levels : $7e$, $5a_1$, $8e$, $9e$, and $6a_1$. The multiplet configurations are obtained from one-electron calculations.

Complex	N	Electronic configuration	Spin	Multiplet
$(\mathrm{Au}_s\mathrm{Ti}_i)^+$	6	$5a_{1\uparrow}^1\ 7e_\uparrow^2\ 7e_\downarrow^2\ 8e_\uparrow^1\ 6a_{1\uparrow}^0\ 9e_\uparrow^0$	1	^3E
$(\mathrm{Au}_s\mathrm{Ti}_i)^0$	7	$5a_{1\uparrow}^1\ 7e_\uparrow^2\ 7e_\downarrow^2\ 8e_\uparrow^2\ 6a_{1\uparrow}^0\ 9e_\uparrow^0$	3/2	^4A
$(\mathrm{Au}_s\mathrm{Ti}_i)^-$	8	$5a_{1\uparrow}^1\ 7e_\uparrow^2\ 7e_\downarrow^2\ 8e_\uparrow^2\ 6a_{1\uparrow}^1\ 9e_\uparrow^0$	2	$^5A_1$
$(\mathrm{Au}_s\mathrm{Ti}_i)^-$	8	$5a_{1\uparrow}^1\ 7e_\uparrow^2\ 7e_\downarrow^2\ 8e_\uparrow^2\ 9e_\uparrow^1\ 6a_{1\uparrow}^0$	2	^5E
$(\mathrm{Au}_s\mathrm{V}_i)^+$	7	$5a_{1\uparrow}^1\ 7e_\uparrow^2\ 7e_\downarrow^2\ 8e_\uparrow^2\ 6a_{1\uparrow}^0\ 9e_\uparrow^0$	3/2	^4A
$(\mathrm{Au}_s\mathrm{V}_i)^0$	8	$7e_\uparrow^2\ 5a_{1\uparrow}^1\ 8e_\uparrow^2\ 7e_\downarrow^2\ 5a_{1\downarrow}^1\ 9e_\uparrow^0$	1	$^3A_1$
$(\mathrm{Au}_s\mathrm{V}_i)^-$	9	$7e_\uparrow^2\ 5a_{1\uparrow}^1\ 8e_\uparrow^2\ 7e_\downarrow^2\ 5a_{1\downarrow}^1\ 9e_\uparrow^1\ 6a_{1\uparrow}^0$	3/2	^4E
$(\mathrm{Au}_s\mathrm{Cr}_i)^+$	8	$5a_{1\uparrow}^1\ 7e_\uparrow^2\ 8e_\uparrow^2\ 7e_\downarrow^2\ 5a_{1\downarrow}^1\ 9e_\uparrow^0\ 8e_\downarrow^0$	1	$^3A_1$
$(\mathrm{Au}_s\mathrm{Cr}_i)^0$	9	$5a_{1\uparrow}^1\ 7e_\uparrow^2\ 8e_\uparrow^2\ 5a_{1\downarrow}^1\ 7e_\downarrow^2\ 9e_\uparrow^1\ 8e_\downarrow^0$	3/2	^4E
$(\mathrm{Au}_s\mathrm{Cr}_i)^-$	10	$7e_\uparrow^2\ 5a_{1\uparrow}^1\ 8e_\uparrow^2\ 5a_{1\downarrow}^1\ 7e_\downarrow^2\ 9e_\uparrow^2\ 8e_\downarrow^0$	2	^5A
$(\mathrm{Au}_s\mathrm{Mn}_i)^+$	9	$5a_{1\uparrow}^1\ 7e_\uparrow^2\ 8e_\uparrow^2\ 5a_{1\downarrow}^1\ 7e_\downarrow^2\ 9e_\uparrow^1\ 8e_\downarrow^0$	3/2	^4E
$(\mathrm{Au}_s\mathrm{Mn}_i)^0$	10	$5a_{1\uparrow}^1\ 7e_\uparrow^2\ 8e_\uparrow^2\ 5a_{1\downarrow}^1\ 7e_\downarrow^2\ 9e_\uparrow^2\ 8e_\downarrow^0$	2	^5A
$(\mathrm{Au}_s\mathrm{Mn}_i)^-$	11	$5a_{1\uparrow}^1\ 7e_\uparrow^2\ 8e_\uparrow^2\ 5a_{1\downarrow}^1\ 7e_\downarrow^2\ 9e_\uparrow^2\ 8e_\downarrow^1\ 6a_{1\downarrow}^0$	3/2	^4E
$(\mathrm{Au}_s\mathrm{Mn}_i)^-$	11	$5a_{1\uparrow}^1\ 7e_\uparrow^2\ 8e_\uparrow^2\ 5a_{1\downarrow}^1\ 7e_\downarrow^2\ 9e_\uparrow^2\ 6a_{1\downarrow}^1\ 8e_\downarrow^0$	5/2	$^6A_1$
$(\mathrm{Au}_s\mathrm{Fe}_i)^+$	10	$5a_{1\uparrow}^1\ 5a_{1\downarrow}^1\ 7e_\uparrow^2\ 7e_\downarrow^2\ 8e_\uparrow^2\ 8e_\downarrow^2\ 9e_\uparrow^0\ 9e_\downarrow^0$	0	$^1A_1$
$(\mathrm{Au}_s\mathrm{Fe}_i)^0$	11	$5a_{1\uparrow}^1\ 5a_{1\downarrow}^1\ 7e_\uparrow^2\ 7e_\downarrow^2\ 8e_\uparrow^2\ 8e_\downarrow^2\ 9e_\uparrow^1\ 6a_{1\uparrow}^0$	1/2	^2E
$(\mathrm{Au}_s\mathrm{Fe}_i)^-$	12	$7e_\uparrow^2\ 5a_{1\uparrow}^1\ 5a_{1\downarrow}^1\ 8e_\uparrow^2\ 7e_\downarrow^2\ 9e_\uparrow^2\ 8e_\downarrow^2\ 6a_{1\uparrow}^0$	1	^3A

B. Spin-unrestricted electronic structure of the Si:$\mathrm{Au}_s TM_i$ systems (TM=Ti, V, Cr, Mn, and Fe)

Table I shows the *spin-unrestricted* single-particle configuration for the gap energy levels of the negative, neutral, and positive $\mathrm{Au}_s TM_i$ trigonal complexes in Si, with TM =Ti, V, Cr, Mn, and Fe. The level ordering is that of increasing energy. The ''up'' and ''down'' spins are represented by ↑ and ↓ arrows, respectively. The spin counterparts of these levels, which are unoccupied and located in the Si conduction band, are not shown. The table also displays the total number of electrons (N) filling these gap levels, the spin of the centers (S), and the multiplet configuration obtained from one-electron calculations.

As can be verified from Table I, most of the complexes in positive, neutral, and negative charge states have a nondegenerated multiplet ground state, with angular momentum $L=0$. Therefore, they are stable configurations in trigonal symmetry. Those complexes in a certain charge state, which present a degenerated ground-state multiplet, will be analyzed case by case.

For the $(\mathrm{Au}_s\mathrm{Ti}_i)^+$ complex, the ground state is degenerated. The highest occupied energy level ($8e_\uparrow^1$) presents a $3d$ character, so that a JT distortion is expected. In this case, distortions must be considered in the calculations in order to realistically describe this charge state. For the $(\mathrm{Au}_s\mathrm{Ti}_i)^-$ complex, two electronic configurations are found, with the total energy difference between them lower than 0.1 eV, inside the error of the theoretical model. Both configurations have total spin $S=2$. The one that has ^5E ground state, with the highest occupied energy level ($9e_\uparrow^1$) displaying a Ti-$3d$ character, is a possible active JT center. Therefore, the configuration having $^5A_1$ ground state is the only stable one in a trigonal symmetry.

For the $(\mathrm{Au}_s\mathrm{V}_i)^-$ ($N=9$) complex, although the results show a degenerated ^4E ground state, the highest occupied energy level ($9e_\uparrow^1$) has a delocalized character, possibly inhibiting a JT distortion. In this case, distortions are expected to be small or absent due to the delocalized character of the $9e_\uparrow$ level. The angular momentum is expected to be quenched and the center would be stable in trigonal symmetry.

For the $(\mathrm{Au}_s\mathrm{Cr}_i)^0$ and $(\mathrm{Au}_s\mathrm{Mn}_i)^+$ ($N=9, S=3/2$) pairs, the stability analysis is the same as the one for the $(\mathrm{Au}_s\mathrm{V}_i)^-$ complex. Our theoretical analysis is consistent with EPR experimental measurements,[1] which found both complexes in trigonal symmetry and total angular momentum $J=3/2$.

For the $(\mathrm{Au}_s\mathrm{Mn}_i)^-$, two electronic configurations are found, each one giving a different total spin ($S=3/2$ or 5/2). The one giving ^4E ground state, having the highest occupied energy level ($8e_\downarrow^1$) with a strong Mn_i-$3d$ character, is an active JT center. On the other hand, the one giving an orbital singlet $^6A_1$ ground state indicates that the system does not undergo JT distortions and matches well the EPR results.[1]

For the $(\mathrm{Au}_s\mathrm{Fe}_i)^0$ pair the ground state is an ^2E multiplet. The $9e$ level exchange splitting is such that the $9e_\uparrow$ level presents higher energy than the $8e_\downarrow$ level, driving the complex to a low spin configuration. Although this result indicates that the defect is an active JT center, one can conclude that distortions are expected to be small or absent since the unpaired electron is occupying a delocalized state ($9e_\uparrow^1$). Therefore, the angular momentum is expected to be quenched and the effective spin of the center would be $S=1/2$. These observations are consistent with EPR results.[8]

The different spin configurations of the complexes, as shown in Table I, do not arise from a magnetic coupling

TABLE II. Experimental Fermi contact term in the Au and TM nuclei for $\mathrm{Au}_s TM_i$ trigonal complexes in Si, in units of 10^{-4} cm^{-1}. J is the observed effective total angular momentum of the centers.

Complex	J	Au $A_\parallel$	Au $A_\perp$	TM $A_\parallel$	TM $A_\perp$
$(\mathrm{Au}_s\mathrm{Cr}_i)^0$ [a]	3/2	+4.5	+2.6	+10.9	+9.1
$(\mathrm{Au}_s\mathrm{Mn}_i)^+$ [a]	3/2	+3.9	+2.0	−60.4	−48.1
$(\mathrm{Au}_s\mathrm{Mn}_i)^-$ [a]	5/2	±1.1	[−4.0,4.0]	±41.0	±38.4
$(\mathrm{Au}_s\mathrm{Fe}_i)^0$ [b]	1/2	±15.1	±9.2	±3.3	±5.6

[a]Reference 1.
[b]Reference 8.

between the independent impurities but originate from different electronic populations of the molecular orbitals of the complexes.

Another important observation can be extracted from the results shown in Table I related to the $(\mathrm{Au}_s\mathrm{Cr}_i)^-$, $(\mathrm{Au}_s\mathrm{Mn}_i)^0$, and $(\mathrm{Au}_s\mathrm{Fe}_i)^+$ pairs, all having $N=10$. The exchange splitting is such that it drives the $(\mathrm{Au}_s\mathrm{Cr}_i)^-$ and $(\mathrm{Au}_s\mathrm{Mn}_i)^0$ centers to high spin configurations, while it drives the $(\mathrm{Au}_s\mathrm{Fe}_i)^+$ center to a low spin configuration. It is worth mentioning that computational simulations were also attempted assuming a low spin configuration for $(\mathrm{Au}_s\mathrm{Cr}_i)^-$ and $(\mathrm{Au}_s\mathrm{Mn}_i)^0$ pairs, and a high spin configuration for $(\mathrm{Au}_s\mathrm{Fe}_i)^+$ complex. These results indicated that $(\mathrm{Au}_s\mathrm{Cr}_i)^-$ with $S=0$ and $(\mathrm{Au}_s\mathrm{Fe}_i)^+$ with $S=2$ and $S=1$ are excited states, i.e., they present unoccupied energy levels below occupied ones. For $(\mathrm{Au}_s\mathrm{Mn}_i)^0$ the low spin configuration ($S=0$) is 0.5 eV higher in energy than the high spin one ($S=2$).

We have also simulated the electronic structure of the $(\mathrm{Au}_s\mathrm{Fe}_i)^0$ pair for the nondegenerated multiplet state ($^2A_1$), in C_{3v} symmetry, by transferring the electron from the highest spin up energy level ($9e_\uparrow$) to the unoccupied lowest spin up energy level ($6a_\uparrow$). The calculations indicate that this configuration corresponds to an excited state, giving a total energy 0.3 eV higher than the one presented in Table I, in disagreement with LMTO-ASA (linear muffin-tin orbitals method in the atomic spheres approximation) results.[42]

For $\mathrm{Au}_s TM_i$ complexes, along the $3d$ series in the Periodic Table, with $TM=\mathrm{Mn}$ and below it, they show a high spin configuration, while for $TM=\mathrm{Fe}$ and over it, the pairs present a low spin configuration. This conclusion is consistent with our results for complexes involving Ni and Co, which were analyzed as having low spin configurations. Therefore, while going from Mn to Fe there is a transition related to the exchange splitting. According to these results, the electronic configurations, which determine the electrical, optical, and magnetic properties of the complex ground states, are defined by high effective spin from Ti to Mn and by low effective spin configurations from Fe to Co.

C. Hyperfine parameters and transition energies

The *spin-unrestricted* calculations allow us to access the values of the Fermi hyperfine contact energy at the impurities and silicon nuclei. In this section we present results of the hyperfine parameters and transition energies for the $\mathrm{Au}_s TM_i$ trigonal pairs in Si, with $TM=\mathrm{Ti}$, V, Cr, Mn, and Fe. We consider only those complexes that are found to be stable in trigonal symmetry, as discussed in the preceding section.

Table II presents the available experimental results for the effective total angular momentum and the Fermi contact term in the Au and TM nuclei for the $\mathrm{Au}_s TM_i$ complexes in trigonal symmetry.[1,8] Table III displays the theoretical Fermi contact terms in the Au_s, TM_i, and Si (first neighbors to the TM_i impurities) nuclei for neutral, positive, and negative $\mathrm{Au}_s TM_i$ trigonal complexes in Si. The experimental results for the Fermi contact terms are presented in parentheses, considering the several possible values due to the uncertainty in the sign of some measurements.

For the $(\mathrm{Au}_s\mathrm{Cr}_i)^0$ and $(\mathrm{Au}_s\mathrm{Mn}_i)^+$ pairs, the theoretical results are in excellent agreement with the experimental

TABLE III. Theoretical effective spin and Fermi contact terms in the Au^{197}, TM^*, and Si^{29} nuclei, for neutral, positive, and negative $\mathrm{Au}_s TM_i$ trigonal complexes in Si, in units of 10^{-4} cm^{-1}. The numbers in parentheses are found using experimental results presented in Table II by using $a=1/3A_\parallel+2/3A_\perp$. For those experimental results in which the sign of either $A_\parallel$ or $A_\perp$ is not known, the values in parentheses are obtained assuming $(\mathrm{sgn}A_\parallel)=(\mathrm{sgn}A_\perp)$ and $(\mathrm{sgn}A_\parallel)=-(\mathrm{sgn}A_\perp)$. ($^*\mathrm{Ti}^{49}$, V^{51}, Cr^{53}, Mn^{55}, Fe^{57}.)

Complex	Effective spin	Multiplet	a(Au)	$a(TM)$	a(Si)
$(\mathrm{Au}_s\mathrm{Ti}_i)^0$	3/2	^4A	+1.7	+21.3	+25.3
$(\mathrm{Au}_s\mathrm{Ti}_i)^-$	2	$^5A_1$	+0.4	+8.1	+36.6
$(\mathrm{Au}_s\mathrm{V}_i)^+$	3/2	^4A	+4.1	+242.4	+17.4
$(\mathrm{Au}_s\mathrm{V}_i)^0$	1	$^3A_1$	+2.5	−141.9	+24.4
$(\mathrm{Au}_s\mathrm{V}_i)^-$	3/2	^4E	+0.8	−149.5	+29.1
$(\mathrm{Au}_s\mathrm{Cr}_i)^+$	1	$^3A_1$	+2.9	+25.8	+22.4
$(\mathrm{Au}_s\mathrm{Cr}_i)^0$	3/2	^4E	+1.3 (+3.2)	+10.8 (+9.7)	+25.1
$(\mathrm{Au}_s\mathrm{Cr}_i)^-$	2	^5A	+2.5	−31.2	−24.2
$(\mathrm{Au}_s\mathrm{Mn}_i)^+$	3/2	^4E	+0.9 (+2.6)	−81.2 (−52.2)	+17.7
$(\mathrm{Au}_s\mathrm{Mn}_i)^0$	2	^5A	+4.2	+101.4	−20.0
$(\mathrm{Au}_s\mathrm{Mn}_i)^-$	5/2	$^6A_1$	−4.2 ([−3.0,3.0])	−62.1 (±11.9,±39.3)	+6.4
$(\mathrm{Au}_s\mathrm{Fe}_i)^0$	1/2	^2E	−2.5 (±1.1,±11.1)	−5.3 (±2.6,±4.8)	+7.7
$(\mathrm{Au}_s\mathrm{Fe}_i)^-$	1	^3A	−3.2	+11.2	+8.2

TABLE IV. Experimental acceptor and donor energy transitions and Mott-Hubbard potentials (U_{expt} and U_{theor}) for $\mathrm{Au}_s TM_i$ trigonal complexes in Si. All values are given in eV, and the gap energy of crystalline Si is assumed to be $E_g = 1.12$ eV.

	Experimental values			Theoretical value
Complex	Acceptor	Donor	U_{expt}	U_{theor}
$\mathrm{Au}_s\mathrm{Ti}_i$				<0.75
$\mathrm{Au}_s\mathrm{V}_i$	$E_c - 0.20$ [a]	$E_v + 0.42$ [a]	0.50	0.56
$\mathrm{Au}_s\mathrm{Cr}_i$		$E_v + 0.35$ [a]		0.44
$\mathrm{Au}_s\mathrm{Mn}_i$	$E_c - 0.24$ [a]	$E_v + 0.57$ [a]	0.31	0.45
$\mathrm{Au}_s\mathrm{Fe}_i$	$E_c - 0.354$ [b]	$E_v + 0.434$ [b]	0.332	0.42

[a]Reference 12.
[b]Reference 11.

data.[1] For the $(\mathrm{Au}_s\mathrm{Mn}_i)^-$ and $(\mathrm{Au}_s\mathrm{Fe}_i)^0$ pairs, a simple comparison with experimental data[1,8] could be misleading, although the theoretical results agree reasonably well with some of the possible values. The effective spin values for these centers are in excellent agreement with experimental effective total angular momentum (J) shown in Table II.

Although there are not many experimental results for the Fermi contact term, our theoretical values may serve as a guideline for future investigations of these complexes.

Table IV presents the experimental acceptor and donor transition energies and Mott-Hubbard potentials (U_{expt} and U_{theor}) for the $\mathrm{Au}_s TM_i$ trigonal pairs in Si (TM = Ti, V, Cr, Mn, and Fe). The potential is computed assuming for the crystalline Si an energy gap (E_g) of 1.12 eV.

For $\mathrm{Au}_s\mathrm{Ti}_i$ complex the theoretical Mott-Hubbard potential value is an overestimation. This is because the donor transition involves a final state with strong Ti-3d localized atomic character, requiring the inclusion of structural distortions in order to describe the final state. For all other complexes, the theoretical values are in good agreement with the experimental Mott-Hubbard potentials. The value of U_{theor} for the $\mathrm{Au}_s\mathrm{Cr}_i$ pair and the measured donor transition energy[12] allow us to predict the acceptor transition energy to be around $E_c - 0.33$ eV.

We expect that the theoretical predictions presented in Tables III and IV will motivate further work on these complexes, allowing a more conclusive description of their electronic structure.

IV. FINAL REMARKS

In summary, we have studied the electronic properties of the $\mathrm{Au}_s\mathrm{Ti}_i$, $\mathrm{Au}_s\mathrm{V}_i$, $\mathrm{Au}_s\mathrm{Cr}_i$, $\mathrm{Au}_s\mathrm{Mn}_i$, $\mathrm{Au}_s\mathrm{Fe}_i$, $\mathrm{Au}_s\mathrm{Co}_i$, and $\mathrm{Au}_s\mathrm{Ni}_i$ trigonal complexes in silicon. The results show that the ionic model used to describe the pairs as an interaction between the two impurities in the complex is not valid. Instead, we find that the microscopic model to describe them is essentially covalent and involves not only the molecular orbitals coming from the Au_s and TM_i impurities but also the Si host atoms.

We observe a chemical trend in the properties of the complexes as the TM_i atom changes. First, the orbitals coming from the Au-5d states are very localized and remain in the bottom of the valence band as resonant states, playing an indirect role in determining the electronic, magnetic, and optical properties of the centers. Besides, starting from the interstitial Ni atom in the complex, the gap dangling-bond-like levels, which are degenerated states, split as one proceeds to lighter interstitial impurities, and their charge distribution begins to display a 3d character. On the other hand, the resonant states showing a strong 3d character for interstitial Ni delocalize onto the neighboring Si atoms as one proceeds to lighter impurities. This trend is a consequence of the increasing covalent interaction between the Au_s and the TM_i-3d gap and resonant levels, going from heavier to lighter TM impurities.

The *spin-polarized* one-electron calculations give a comprehensive analysis of the stability of the complexes in trigonal symmetry. Moreover, they show that the exchange splitting drives the $\mathrm{Au}_s\mathrm{Ti}_i$, $\mathrm{Au}_s\mathrm{V}_i$, $\mathrm{Au}_s\mathrm{Cr}_i$, and $\mathrm{Au}_s\mathrm{Mn}_i$ pairs to a high spin configuration, while the $\mathrm{Au}_s\mathrm{Fe}_i$, $\mathrm{Au}_s\mathrm{Co}_i$, and $\mathrm{Au}_s\mathrm{Ni}_i$ complexes are described by a low spin configuration. These spin configurations do not arise from a magnetic coupling between the two spins of the independent impurities, but from the electronic population of the molecular orbitals.

The results for the Fermi contact hyperfine terms, effective spin of the centers, and the Mott-Hubbard potentials are in very good agreement with available EPR and DLTS experimental data, providing a strong support for structural stability analysis and the covalent model suggested by us. Moreover, although lattice distortions were not taken into account, they are not expected to affect the overall picture resulting from the calculations, such as the covalent model and the gap transition energies. This assumption is based on the structural stability analysis related to JT distortions and the agreement with EPR and DLTS experiments for $\mathrm{Au}_s\mathrm{V}_i$, $\mathrm{Au}_s\mathrm{Cr}_i$, $\mathrm{Au}_s\mathrm{Mn}_i$, $\mathrm{Au}_s\mathrm{Fe}_i$, and $\mathrm{Au}_s\mathrm{Ni}_i$ complexes, which ascribe a C_{3v} symmetry for these pairs. Fermi contact hyperfine terms would be the most sensitive parameters to lattice relaxations, which we have not considered. However, the good agreement between theoretical and EPR values provides support to state that lattice relaxations should be small.

The donor-acceptor activities involve delocalized impurity states, equivalent to the isolated gold center, the only exception being the $\mathrm{Au}_s\mathrm{Ti}_i$ complex donor transition. This similarity leads to the conclusion that the conventional multicharge-state model is also applicable to almost all of these complexes.

The understanding of the behavior of TM-related complexes in silicon has progressed rapidly during recent years, and we hope that the results presented here may provide a guideline for further theoretical and experimental investigations of complexes involving transition metals in doped silicon.

ACKNOWLEDGMENTS

We are indebted to Professor A. Fazzio for the critical reading of the manuscript. L.V.C.A. acknowledges partial support from Brazilian Agencies CNPq and FAPESP. J.F.J. acknowledges support from FAPESP.

[1] G. W. Ludwig and H. H. Woodburry, Solid State Phys. **13**, 223 (1962).
[2] A. G. Milnes, *Deep Impurities in Semiconductors* (Wiley, New York, 1973).
[3] H. G. Grimmeiss, Annu. Rev. Mater. Sci. **7**, 341 (1977).
[4] J.-W. Chen and A. G. Milnes, Annu. Rev. Mater. Sci. **10**, 157 (1980).
[5] D. V. Lang, H. G. Grimmeiss, E. Meijer, and M. Jaros, Phys. Rev. B **22**, 3917 (1980).
[6] L-Å. Ledebo and Zhan-Gou Wang, Appl. Phys. Lett. **42**, 680 (1983).
[7] J. Utzig and W. Schröter, Appl. Phys. Lett. **45**, 761 (1984).
[8] R. L. Kleinhenz, Y. H. Lee, J. W. Corbett, E. G. Sieverts, S. H. Muller, and C. A. J. Ammerlaan, Phys. Status Solidi B **108**, 363 (1981).
[9] E. G. Sieverts, S. H. Muller, C. A. J. Ammerlaan, R. L. Kleinheiz, and J. W. Corbett, Phys. Status Solidi B **109**, 83 (1982).
[10] D. Rodewald, S. Severitt, H. Vollmer, and R. Labusch, Solid State Commun. **67**, 573 (1988).
[11] S. D. Brotherton, P. Bradley, A. Gill, and E. R. Weber, J. Appl. Phys. **55**, 952 (1984).
[12] H. Lemke, Phys. Status Solidi A **75**, 473 (1983).
[13] R. Czaputa, Appl. Phys. A: Solids Surf. **49**, 431 (1989).
[14] M. Höhne, Phys. Status Solidi B **99**, 651 (1980); **109**, 525 (1982).
[15] G. D. Watkins, M. Kleverman, A. Thilderkvist, and H. G. Grimmeiss, Phys. Rev. Lett. **67**, 1149 (1991).
[16] M. Kleverman, A. Thilderkvist, G. Grossmann, H. G. Grimmeiss, and G. D. Watkins, Solid State Commun. **93**, 383 (1995).
[17] F. G. Anderson, J. Phys.: Condens. Matter **3**, 4421 (1991).
[18] G. Armelles, J. Barrau, M. Brousseau, B. Pajot, and C. Naud, Solid State Commun. **56**, 303 (1985).
[19] M. Kleverman, J. Olajos, and H. G. Grimmeiss, Phys. Rev. B **35**, 4093 (1987).
[20] D. Thebault, J. Barrau, G. Armelles, N. Lauret, and J. P. Noguier, Phys. Status Solidi B **125**, 357 (1984).
[21] L. V. C. Assali, J. R. Leite, and A. Fazzio, Phys. Rev. B **32**, 8085 (1985).
[22] L. V. C. Assali and J. R. Leite, Solid State Commun. **58**, 577 (1986).
[23] J. R. Leite, V. M. S. Gomes, L. V. C. Assali, and L. M. R. Scolfaro, J. Electron. Mater. **14a**, 885 (1985).
[24] K. H. Johnson, *Advances in Quantum Chemistry* (Academic, New York, 1973), Vol. 7, pp. 143–185.
[25] J. C. Slater, *The Self-Consistent Field for Molecules and Solids* (McGraw-Hill, New York, 1974).
[26] H. Siegert and P. Becker, Acta Crystallogr., Sect. A: Found. Crystallogr. **40**, C340 (1984).
[27] K. Schwarz, Phys. Rev. B **5**, 2466 (1972).
[28] L. Hedin and B. I. Lundqvist, J. Phys. C **4**, 2064 (1971).
[29] D. M. Ceperley and B. J. Alder, Phys. Rev. Lett. **45**, 566 (1980).
[30] A. Fazzio, J. R. Leite, and M. L. de Siqueira, J. Phys. C **12**, 513 (1979); **14**, 3469 (1979).
[31] W. M. Orellana and L. V. C. Assali, Mater. Sci. Forum **143-147**, 779 (1994); Braz. J. Phys. **24**, 390 (1994).
[32] L. V. C. Assali and J. R. Leite, Phys. Rev. Lett. **55**, 980 (1985): Phys. Rev. B **36**, 1296 (1987); Mater. Sci. Forum **38-41**, 409 (1989); **83-87**, 143 (1992).
[33] D. D. Koelling and B. N. Harmon, J. Phys. C **10**, 3107 (1977).
[34] J. H. Wood and A. M. Boring, Phys. Rev. B **18**, 2701 (1978).
[35] J. L. A. Alves, J. R. Leite, V. M. S. Gomes, and L. V. C. Assali, Solid State Commun. **55**, 333 (1985).
[36] A. Fazzio, M. J. Caldas, and A. Zunger, Phys. Rev. B **32**, 934 (1985).
[37] G. G. DeLeo, G. D. Watkins, and W. B. Fowler, Phys. Rev. B **23**, 1851 (1981); **25**, 4962 (1982); **25**, 4972 (1982).
[38] F. Beeler, O. K. Andersen, and M. Scheffler, Phys. Rev. Lett. **55**, 1498 (1985); Phys. Rev. B **41**, 1603 (1990).
[39] H. Katayama-Yoshida and A. Zunger, Phys. Rev. B **31**, 8317 (1985).
[40] F. D. M. Haldane and P. W. Anderson, Phys. Rev. B **13**, 2553 (1976).
[41] E. R. Weber, Appl. Phys. A: Solids Surf. **30**, 1 (1983).
[42] H. Overhof and H. Weihrich, Mater. Sci. Forum **196-201**, 1357 (1995).